Günter Hofstetter
Günther Meschke
Editors

International Centre for Mechanical Sciences

Numerical Modeling of Concrete Cracking

CISM Courses and Lectures, vol. 532

SpringerWienNewYork

SpringerWienNewYork

CISM COURSES AND LECTURES

The series presents lecture notes, monographs, edited works and proceedings in the field of Mechanics, Engineering, Computer Science and Applied Mathematics.
Purpose of the series is to make known in the international scientific and technical community results obtained in some of the activities organized by CISM, the International Centre for Mechanical Sciences.

INTERNATIONAL CENTRE FOR MECHANICAL SCIENCES

COURSES AND LECTURES - No. 532

NUMERICAL MODELING OF CONCRETE CRACKING

EDITED BY

GÜNTER HOFSTETTER
UNIVERSITY OF INNSBRUCK, AUSTRIA

GÜNTHER MESCHKE
RUHR UNIVERSITY BOCHUM, GERMANY

SpringerWienNewYork

This volume contains 185 illustrations

SPIN 80073533

All contributions have been typeset by the authors.

ISBN 978-3-7091-0896-3 SpringerWienNewYork

PREFACE

Reliable model-based prognoses of the initiation and propagation of cracks in concrete plays an important role for the durability and integrity assessment of concrete and reinforced concrete structures. To this end, a large number of material models for concrete cracking based on different theories (e.g., damage mechanics, fracture mechanics, plasticity theory and combinations of the mentioned theories) as well as advanced finite element methods suitable for the representation of cracks (e.g., the Extended Finite Element Method and Embedded Crack Models) have been developed in recent years.

The focus of the Advanced School on "Numerical Modeling of Concrete Cracking" at the International Centre for Mechanical Sciences (CISM) at Udine in May 2009 was laid on numerical models for describing crack propagation in concrete and their applications to numerical simulations of concrete and reinforced concrete structures. The lectures of this course formed the basis for this book. Its aim is to impart fundamental knowledge of the underlying theories of the different approaches for modelling cracking of concrete and to provide a critical survey of the state-of-the-art in computational concrete mechanics.

This book covers a relatively broad spectrum of topics related to modelling of cracks, including continuum-based and discrete crack models, meso-scale models, advanced discretization strategies to capture evolving cracks based on the concept of finite elements with embedded discontinuities and on the extended finite element method, respectively, and, last but not least, extensions to coupled problems such as hygro-mechanical problems as required in computational durability analyses of concrete structures.

Innsbruck and Bochum,
March 2011,

Günter Hofstetter
University of Innsbruck
Austria

Günther Meschke
Ruhr-University Bochum
Germany

CONTENTS

Damage and Smeared Crack Models

Milan Jirásek
Czech Technical University in Prague, Czech Republic

1 Isotropic Damage Models

Continuum damage mechanics is a constitutive theory that describes the progressive loss of material integrity due to the propagation and coalescence of microcracks, microvoids, and similar defects. These changes in the microstructure lead to a degradation of material stiffness observed on the macroscale. The term "continuum damage mechanics" was first used by Hult in 1972 but the concept of damage had been introduced by Kachanov already in 1958 in the context of creep rupture (Kachanov, 1958) and further developed by Rabotnov (1968); Hayhurst (1972); Leckie and Hayhurst (1974). The simplest version of the isotropic damage model considers the damaged stiffness tensor as a scalar multiple of the initial elastic stiffness tensor, i.e., damage is characterized by a single scalar variable. A general isotropic damage model should deal with two scalar variables corresponding to two independent elastic constants of standard isotropic elasticity. More refined theories take into account the anisotropic character of damage; they represent damage by a family of vectors (Krajcinovic and Fonseka, 1981), by a second-order tensor (Vakulenko and Kachanov, 1971) or, in the most general case, by a fourth-order tensor (Chaboche, 1979). Anisotropic formulations can be based on the principle of strain equivalence (Lemaitre, 1971), or on the principle of energy equivalence (Cordebois and Sidoroff, 1979) (the principle of stress equivalence is also conceptually possible but is rarely used).

In the present chapter, we will focus on isotropic damage models and on smeared crack models, which incorporate anisotropy in a simplified way. Anisotropic damage models based on tensorial description of damage will are treated e.g. in Lemaitre and Desmorat (2005).

1.1 One-Dimensional Damage Model

Damage models work with certain internal variables that characterize the density and orientation of microdefects. To introduce the basic concepts, we start from the case of uniaxial stress. For the present purpose, the material is idealized as a

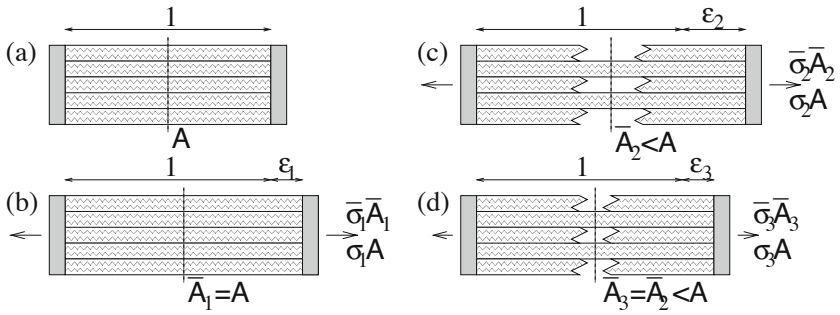

Figure 1. Representation of a uniaxial damage model as a bundle of parallel elastic fibers breaking at different strain levels

bundle of fibers parallel to the direction of loading (Fig. 1a). Initially, all the fibers respond elastically, and the stress is carried by the total cross section of all fibers, A (Fig. 1b). As the applied strain is increased, some fibers start breaking (Fig. 1c). Each fiber is assumed to be perfectly brittle, which means that the stress in the fiber drops down to zero immediately after a critical strain level is reached. However, since the critical strain is different for each fiber, the effective area $\bar{A}$ (i.e., the area of unbroken fibers that can still carry stress) decreases gradually from $\bar{A} = A$ to $\bar{A} = 0$. We have to make a distinction between the *nominal stress* σ, defined as the force per unit initial area of the cross section, and the *effective stress* $\bar{\sigma}$, defined as the force per unit effective area. The nominal stress enters the Cauchy equations of equilibrium on the macroscopic level, while the effective stress is the "true" stress acting in the material microstructure.[1] From the condition of equivalence, $\sigma A = \bar{\sigma}\bar{A}$, we obtain

$$\sigma = \frac{\bar{A}}{A}\bar{\sigma} \tag{1}$$

The ratio of the effective area to the total area, $\bar{A}/A$, is a scalar characterizing the *integrity* of the material. In damage mechanics it is customary to work with the *damage variable* defined as

$$D = 1 - \frac{\bar{A}}{A} = \frac{A - \bar{A}}{A} = \frac{A_d}{A} \tag{2}$$

where $A_d = A - \bar{A}$ is the damaged part of the area. An intact (undamaged) material is characterized by $\bar{A} = A$, i.e., by $D = 0$. Due to propagation of microdefects and

[1] Of course, detailed micromechanical analysis would reveal local oscillations of the stress fields dependent on the specific defect geometry, and the representation of the actual stress distribution by one averaged value—the effective stress—is just a simplification for modeling purposes.

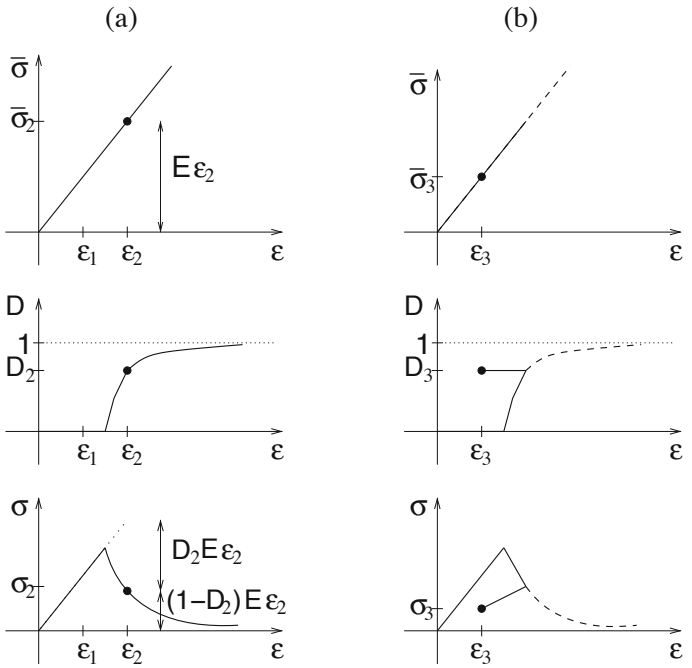

Figure 2. Evolution of effective stress $\bar{\sigma}$, damage variable D and nominal stress σ under a) monotonic loading, b) non-monotonic loading

their coalescence, the damage variable grows and at late stages of the degradation process it attains or asymptotically approaches the limit value $D = 1$, corresponding to a completely damaged material with effective area reduced to zero. In the simplest version of the model, each fiber is supposed to remain linear elastic up to the strain level at which it breaks.[2] Consequently, the effective stress $\bar{\sigma}$ is governed by Hooke's law,

$$\bar{\sigma} = E\varepsilon \tag{3}$$

Combining (1)–(3) we obtain the constitutive law for the nominal stress,

$$\sigma = (1 - D)E\varepsilon \tag{4}$$

Damage evolution can be characterized by the dependence of the damage variable on the applied strain,

$$D = g(\varepsilon) \tag{5}$$

[2]In general, the fictitious "fibers" can obey any (nonlinear) constitutive law, which provides one possible framework for coupling of damage with other dissipative phenomena, such as plasticity.

Function g affects the shape of the stress-strain diagram and can be directly identified from a uniaxial test. The evolution of the effective stress, damage variable, and nominal stress in a material that remains elastic up to the peak stress is shown in Fig. 2a. This description is valid only for monotonic loading by an increasing applied strain ε. When the material is first stretched up to a certain strain level ε_2 that induces damage $D_2 = g(\varepsilon_2)$ and then the strain decreases (Fig. 1d), the damaged area remains constant and the material responds as an elastic material with a reduced Young's modulus $E_2 = (1 - D_2)E$. This means that, during unloading and partial reloading, the damage variable in (4) must be evaluated from the largest previously reached strain and not from the current strain ε. It is convenient to introduce an internal variable κ characterizing the maximum strain level reached in the previous history of the material up to a given time t, i.e., to set

$$\kappa(t) = \max_{\tau \leq t} \varepsilon(\tau) \tag{6}$$

where t is not necessarily the physical time—it can be any monotonically increasing parameter controling the loading process. The damage evolution law (5) is then replaced by equation

$$D = g(\kappa) \tag{7}$$

that remains valid not only during monotonic loading but also during unloading and reloading. The evolution of the effective stress, damage variable, and nominal stress in a non-monotonic test is shown in Fig. 2b. Note that, upon a complete removal of the applied stress, the strain returns to zero (due to elasticity of the yet unbroken fibers), i.e., the pure damage model does not take into account any permanent strains. Nevertheless, the material state is different from the initial virgin state, because the damage variable is not zero and the stiffness and strength mobilized in a new tensile loading process are smaller than their initial values. The loading history is reflected by the value of the damage variable D.

To gain further insight, we rewrite the constitutive law (4) in the form $\sigma = E_s\varepsilon$ where $E_s = (1-D)E$ is the apparent (damaged) modulus of elasticity. Instead of defining the variable κ through (6), we introduce a loading function $f(\varepsilon, \kappa) = \varepsilon - \kappa$ and postulate the loading-unloading conditions in the Kuhn-Tucker form,

$$f \leq 0, \qquad \dot{\kappa} \geq 0, \qquad \dot{\kappa} f = 0 \tag{8}$$

The first condition means that κ can never be smaller than ε, and the second condition means that κ cannot decrease. Finally, according to the third condition, κ can grow only if the current values of ε and κ are equal.

The basic ingredients of the uniaxial damage theory are summarized as follows:

- the stress-strain law in the secant format,

$$\sigma = E_s\varepsilon \tag{9}$$

- the equation relating the apparent stiffness to the damage variable,

$$E_s = (1 - D)E \tag{10}$$

- the law governing the evolution of the damage variable,

$$D = g(\kappa) \tag{11}$$

- the loading function

$$f(\varepsilon, \kappa) = \varepsilon - \kappa \tag{12}$$

  specifying the elastic domain $\mathcal{E}_\kappa = \{\varepsilon \mid f(\varepsilon, \kappa) < 0\}$, i.e., the set of states for which damage does not grow, and
- the loading-unloading conditions (8).

1.2 Damage Models with Strain-Based Loading Functions

Simple Models with One Damage Variable. The simplest extension of the uniaxial damage theory to general multiaxial stress states is achieved by the isotropic damage model with a single scalar variable. Isotropic damage models are based on the simplifying assumption that the stiffness degradation is isotropic, i.e., stiffness moduli corresponding to different directions decrease proportionally, independently of the direction of loading. Since an isotropic elastic material is characterized by two independent elastic constants, a general isotropic damage model should deal with two damage variables. The model with a single variable makes use of an additional assumption that the relative reduction of all the stiffness coefficients is the same, in other words, that the Poisson ratio is not affected by damage. Consequently, the damaged stiffness tensor is expressed as

$$\mathbb{E}_S = (1 - D)\,\mathbb{E} \tag{13}$$

where $\mathbb{E}$ is the elastic stiffness tensor of the intact material, and D is the damage variable. In the present context, $\mathbb{E}_S$ is the secant stiffness that relates the total strain to total stress, according to the formula

$$\boldsymbol{\sigma} = \mathbb{E}_S : \boldsymbol{\varepsilon} = (1 - D)\,\mathbb{E} : \boldsymbol{\varepsilon} \tag{14}$$

Clearly, (13) is a generalization of (10), and (14) is a generalization of (9) and (4). In terms of the *effective stress tensor*, defined as

$$\overline{\boldsymbol{\sigma}} = \mathbb{E} : \boldsymbol{\varepsilon} \tag{15}$$

equation (14) can alternatively be written as

$$\boldsymbol{\sigma} = (1 - D)\,\overline{\boldsymbol{\sigma}} \tag{16}$$

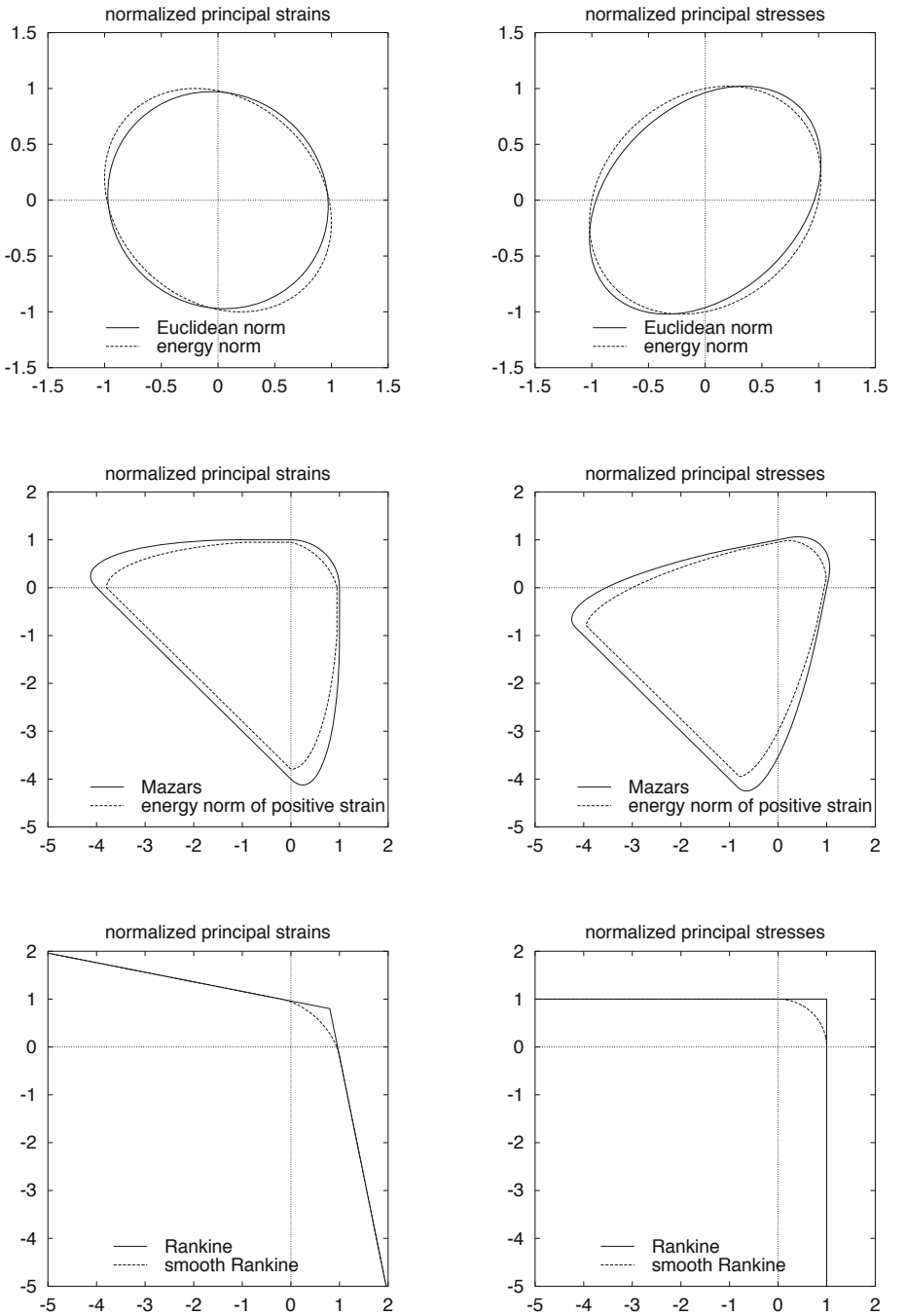

Figure 3. Loading surfaces for various definitions of equivalent strain

which is the multidimensional generalization of (1).

Similar to the uniaxial case, we introduce a loading function f specifying the elastic domain and the states at which damage grows. The loading function now depends on the strain tensor, $\boldsymbol{\varepsilon}$, and on a variable κ that controls the evolution of the elastic domain. Physically, κ is a scalar measure of the largest strain level ever reached in the history of the material. States for which $f(\boldsymbol{\varepsilon}, \kappa) < 0$ are supposed to be below the current damage threshold. Damage can grow only if the current state reaches the boundary of the elastic domain. This is described by the loading-unloading conditions (8). It is convenient to postulate the loading function in the form

$$f(\boldsymbol{\varepsilon}, \kappa) = \tilde{\varepsilon}(\boldsymbol{\varepsilon}) - \kappa \tag{17}$$

where $\tilde{\varepsilon}$ is the *equivalent strain*, i.e., a scalar measure of the strain level.

In some sense, the expression defining the equivalent strain plays a role similar to the yield function in plasticity, because it directly affects the shape of the elastic domain. The simplest choice is to define the equivalent strain as the Euclidean norm of the strain tensor,

$$\tilde{\varepsilon} = \|\boldsymbol{\varepsilon}\| = \sqrt{\boldsymbol{\varepsilon} : \boldsymbol{\varepsilon}} = \sqrt{\varepsilon_{ij}\varepsilon_{ij}} \tag{18}$$

or as the energy norm,

$$\tilde{\varepsilon} = \sqrt{\frac{\boldsymbol{\varepsilon} : \mathbb{E} : \boldsymbol{\varepsilon}}{E}} = \sqrt{\frac{1}{E} E_{ijkl}\varepsilon_{ij}\varepsilon_{kl}} \tag{19}$$

where E_{ijkl} are the components of the elastic stiffness tensor $\mathbb{E}$ and normalization by Young's modulus E is introduced in order to obtain a strain-like quantity. Each particular definition of equivalent strain corresponds to a certain shape of the elastic domain in the strain space and can be transformed into the stress space. For illustration, Fig. 3(top) shows the elastic domains in projection onto the principal strain plane and in the principal stress plane for the case of plane stress and Poisson's ratio $\nu = 0.2$. The domains are elliptical and symmetric with respect to the origin. Consequently, there would be no difference in the response to tensile and compressive loadings.

For concrete and other materials with very different behaviors in tension and in compression, it is necessary to adjust the definition of equivalent strain. Microcracks in concrete grow mainly if the material is stretched, and so it is natural to take into account only normal strains that are positive and neglect those that are negative. This leads to the so-called Mazars definition of equivalent strain (Mazars, 1984)

$$\tilde{\varepsilon} = \|\langle\boldsymbol{\varepsilon}\rangle\| = \sqrt{\langle\boldsymbol{\varepsilon}\rangle : \langle\boldsymbol{\varepsilon}\rangle} \tag{20}$$

or to its energetic counterpart,

$$\tilde{\varepsilon} = \sqrt{\frac{\langle \boldsymbol{\varepsilon} \rangle : \mathbb{E} : \langle \boldsymbol{\varepsilon} \rangle}{E}} \tag{21}$$

where McAuley brackets $\langle . \rangle$ denote the "positive part" operator. For scalars, $\langle x \rangle = \max(0, x)$, i.e., $\langle x \rangle = x$ for x positive and $\langle x \rangle = 0$ for x negative. For symmetric tensors, such as the strain tensor $\boldsymbol{\varepsilon}$, the positive part is a tensor having the same principal directions $\boldsymbol{n}_I$ as the original one, with principal values ε_I replaced by their positive parts $\langle \varepsilon_I \rangle$. The subscript I ranges from 1 to 3 (the number of spatial dimensions) but it is not subject to Einstein's summation convention because the principal strains ε_I are not components of a first-order tensor. In terms of the spectral decomposition

$$\boldsymbol{\varepsilon} = \sum_{I=1}^{3} \varepsilon_I \, \boldsymbol{n}_I \otimes \boldsymbol{n}_I \tag{22}$$

the positive part of $\boldsymbol{\varepsilon}$ is expressed as

$$\langle \boldsymbol{\varepsilon} \rangle = \sum_{I=1}^{3} \langle \varepsilon_I \rangle \, \boldsymbol{n}_I \otimes \boldsymbol{n}_I \tag{23}$$

Since $(\boldsymbol{n}_I \otimes \boldsymbol{n}_I) : (\boldsymbol{n}_J \otimes \boldsymbol{n}_J) = \delta_{IJ} =$ Kronecker's delta, definition (20) can be rewritten as

$$\tilde{\varepsilon} = \sqrt{\sum_{I=1}^{3} \langle \varepsilon_I \rangle^2} \tag{24}$$

The elastic domains corresponding to (20) and (21) are shown in Fig. 3(center).

If a model corresponding to the Rankine criterion of maximum principal stress is desired, one may use the definitions

$$\tilde{\varepsilon} = \frac{1}{E} \max_{I=1,2,3} \langle \mathbb{E} : \boldsymbol{\varepsilon} \rangle_I = \frac{1}{E} \max_{I=1,2,3} \langle \overline{\sigma}_I \rangle \tag{25}$$

or

$$\tilde{\varepsilon} = \frac{1}{E} \| \langle \mathbb{E} : \boldsymbol{\varepsilon} \rangle \| = \frac{1}{E} \sqrt{\sum_{I=1}^{3} \langle \mathbb{E} : \boldsymbol{\varepsilon} \rangle_I^2} = \frac{1}{E} \sqrt{\sum_{I=1}^{3} \langle \overline{\sigma}_I \rangle^2} \tag{26}$$

where $\langle \overline{\sigma}_I \rangle = \langle \mathbb{E} : \boldsymbol{\varepsilon} \rangle_I$, $I = 1, 2, 3$, are the positive parts of principal values of the effective stress tensor (15). The former definition exactly corresponds to the Rankine criterion while the latter rounds off the corners in the octants with more than one positive principal stress; see Fig. 3(bottom).

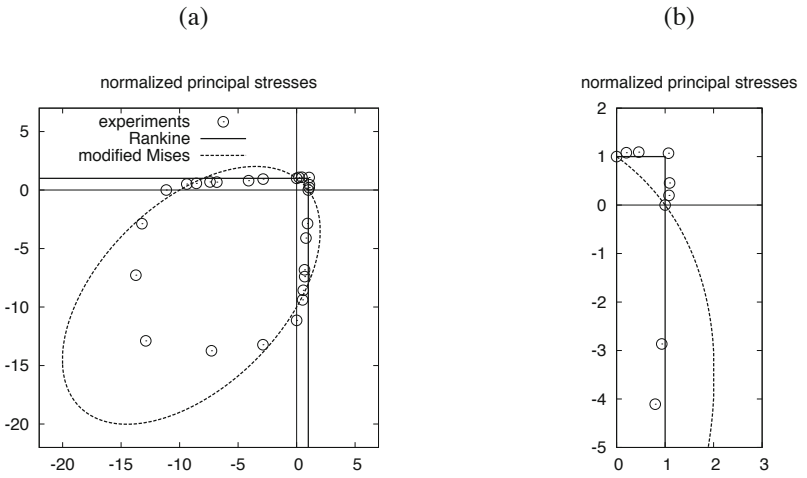

Figure 4. Biaxial strength envelope for concrete and its approximation by isotropic damage models with Rankine and modified Mises definition of equivalent strain

An alternative formula, called the modified von Mises definition (de Vree et al., 1995), reads

$$\tilde{\varepsilon} = \frac{(k-1)I_{1\varepsilon}}{2k(1-2\nu)} + \frac{1}{2k}\sqrt{\frac{(k-1)^2}{(1-2\nu)^2}I_{1\varepsilon}^2 + \frac{12kJ_{2\varepsilon}}{(1+\nu)^2}} \tag{27}$$

where

$$I_{1\varepsilon} = \mathbf{1} : \boldsymbol{\varepsilon} = 3\,\varepsilon_V \tag{28}$$

is the first strain invariant (trace of the strain tensor),

$$J_{2\varepsilon} = \tfrac{1}{2}\mathbf{e} : \mathbf{e} = \tfrac{1}{2}\boldsymbol{\varepsilon} : \boldsymbol{\varepsilon} - \tfrac{1}{6}I_{1\varepsilon}^2 \tag{29}$$

is the second deviatoric strain invariant, and k is a model parameter that sets the ratio between the uniaxial compressive strength f_c and uniaxial tensile strength f_t. The elastic domains corresponding to the modified von Mises definition have ellipsoidal shapes but their centers are shifted from the origin along the hydrostatic axis (except for the special case with parameter $k = 1$, which corresponds to the standard von Mises definition, with equivalent strain proportional to $\sqrt{J_{2\varepsilon}}$).

The uniaxial tensile strength and uniaxial compressive strength can be fitted, but the shape of the elastic domain in the tension-compression quadrant of the principal stress plane does not correspond to experimental data for concrete (Kupfer et al., 1969) and the shear strength is overestimated, see Fig. 4.

An important advantage of isotropic damage models is that the stress evaluation algorithm is usually explicit, without the need for an iterative solution of one or more nonlinear equations. The choice of a loading function in the form (17) endows the variable κ with the meaning of the largest value of equivalent strain that has ever occured in the previous deformation history of the material up to its current state; cf. (8). In other words, (6) can be generalized to

$$\kappa(t) = \max_{\tau \le t} \tilde{\varepsilon}(\tau) \tag{30}$$

For a prescribed strain increment, the corresponding stress is evaluated simply by computing the current value of equivalent strain, updating the maximum previously reached equivalent strain and the damage variable, and reducing the effective stress according to (14). Depending on the definition of equivalent strain one may have to extract the principal strains or principal stresses. This can be done very easily, since closed-form formulas for the eigenvalues of symmetric matrices of size 2×2 or 3×3 are available.

The damaged stiffness tensor $\mathbb{E}_S = (1-D)\mathbb{E}$ introduced in (13) links the total stress to total strain and plays the role of the tangent stiffness only for unloading with constant damage ($f < 0$ or $\dot{f} < 0$). To construct the tangent stiffness tensor for loading with growing damage ($f = 0$ and $\dot{f} = 0$), we need to find the link between stress and strain increments or rates. The damage rate can be expressed in terms of the strain rate using the consistency condition $\dot{f} = 0$ with the rate of the damage loading function evaluated from (17) and combining it with the rate form of equation (11):

$$\dot{D} = \frac{\mathrm{d}g}{\mathrm{d}\kappa}\dot{\kappa} = \frac{\mathrm{d}g}{\mathrm{d}\kappa}\dot{\tilde{\varepsilon}} = \frac{\mathrm{d}g}{\mathrm{d}\kappa}\frac{\partial \tilde{\varepsilon}}{\partial \boldsymbol{\varepsilon}} : \dot{\boldsymbol{\varepsilon}} \tag{31}$$

For convenience, we introduce symbols g' for the derivative $\mathrm{d}g/\mathrm{d}\kappa$ of the damage function, and $\boldsymbol{\eta}$ for the second order tensor $\partial\tilde{\varepsilon}/\partial\boldsymbol{\varepsilon}$ obtained by differentiation of the expression for the equivalent strain with respect to the strain tensor. Substituting $\dot{D} = g'\boldsymbol{\eta} : \dot{\boldsymbol{\varepsilon}}$ into the rate form of the stress-strain law (14) we get

$$\dot{\boldsymbol{\sigma}} = (1-D)\mathbb{E} : \dot{\boldsymbol{\varepsilon}} - \mathbb{E} : \boldsymbol{\varepsilon}\,\dot{D} = (1-D)\mathbb{E} : \dot{\boldsymbol{\varepsilon}} - \bar{\boldsymbol{\sigma}}\,(g'\boldsymbol{\eta} : \dot{\boldsymbol{\varepsilon}}) = \mathbb{E}_{\mathrm{ed}} : \dot{\boldsymbol{\varepsilon}} \tag{32}$$

where $\bar{\boldsymbol{\sigma}} = \mathbb{E} : \boldsymbol{\varepsilon}$ is the effective stress and

$$\mathbb{E}_{\mathrm{ed}} = (1-D)\mathbb{E} - g'\bar{\boldsymbol{\sigma}} \otimes \boldsymbol{\eta} \tag{33}$$

is the elasto-damage stiffness tensor. It is interesting to note that for a model with the equivalent strain based on the energy norm, eq. (19), the tensor $\boldsymbol{\eta}$ is given by

$$\boldsymbol{\eta} = \frac{\partial \tilde{\varepsilon}}{\partial \boldsymbol{\varepsilon}} = \frac{1}{2\sqrt{\dfrac{\boldsymbol{\varepsilon} : \mathbb{E} : \boldsymbol{\varepsilon}}{E}}}\frac{1}{E}2\mathbb{E} : \boldsymbol{\varepsilon} = \frac{\bar{\boldsymbol{\sigma}}}{E\tilde{\varepsilon}} \tag{34}$$

and the resulting elasto-damage stiffness tensor

$$\mathbb{E}_{ed} = (1 - D)\mathbb{E} - \frac{g'}{E\tilde{\varepsilon}}\bar{\boldsymbol{\sigma}} \otimes \bar{\boldsymbol{\sigma}} \tag{35}$$

exhibits major symmetry ($E^{\text{ed}}_{ijkl} = E^{\text{ed}}_{klij}$). For other definitions of equivalent strain, this kind of symmetry is lost.

Mazars Damage Model. A popular damage model specifically designed for concrete was proposed by Mazars (Mazars, 1984, 1986). He introduced two damage variables, D_t and D_c, that are computed from the same equivalent strain (24) using two different damage functions, g_t and g_c. Function g_t is identified from the uniaxial tensile test while g_c corresponds to the compressive test. The damage variable entering the constitutive equations (14) is $D = D_t$ under tension and $D = D_c$ under compression. For general stress states the value of D is obtained as a linear combination

$$D = \alpha_t D_t + \alpha_c D_c \tag{36}$$

where the coefficients α_t and α_c take into account the character of the stress state. In the recent implementation of Mazars model, these coefficients are evaluated as

$$\alpha_t = \left(\sum_{I=1}^{3} \frac{\varepsilon_{tI} \langle \varepsilon_I \rangle}{\tilde{\varepsilon}^2} \right)^{\beta}, \qquad \alpha_c = \left(1 - \sum_{I=1}^{3} \frac{\varepsilon_{tI} \langle \varepsilon_I \rangle}{\tilde{\varepsilon}^2} \right)^{\beta} \tag{37}$$

where ε_{tI}, $I = 1, 2, 3$, are the principal strains due to positive stresses, i.e., the principal values of $\boldsymbol{\varepsilon}_t = \mathbb{C} : \langle \mathbb{E} : \boldsymbol{\varepsilon} \rangle$, in which $\mathbb{C} = \mathbb{E}^{-1}$ is the elastic compliance tensor. The exponent $\beta = 1.06$ slows down the evolution of damage under shear loading (i.e., when principal stresses do not have the same sign). In the original version of the model (Mazars, 1984), β was equal to 1.

Note that if all principal stresses are nonnegative we have $\alpha_t = 1, \alpha_c = 0$, and $D = D_t$, and if all principal stresses are nonpositive we have $\alpha_t = 0, \alpha_c = 1$, and $D = D_c$. These are the "purely tensile" and "purely compressive" stress states. For intermediate stress states the value of D is between D_t and D_c, depending on the relative magnitudes of tensile and compressive stresses. Functions characterizing the evolution of damage were originally proposed in the form (Mazars, 1984)

$$g_t(\kappa) = \begin{cases} 0 & \text{if} \quad \kappa \le \varepsilon_0 \\ 1 - (1 - A_t)\dfrac{\varepsilon_0}{\kappa} - A_t \exp\left[-B_t(\kappa - \varepsilon_0)\right] & \text{if} \quad \kappa \ge \varepsilon_0 \end{cases} \tag{38}$$

$$g_c(\kappa) = \begin{cases} 0 & \text{if} \quad \kappa \le \varepsilon_0 \\ 1 - (1 - A_c)\dfrac{\varepsilon_0}{\kappa} - A_c \exp\left[-B_c(\kappa - \varepsilon_0)\right] & \text{if} \quad \kappa \ge \varepsilon_0 \end{cases} \tag{39}$$

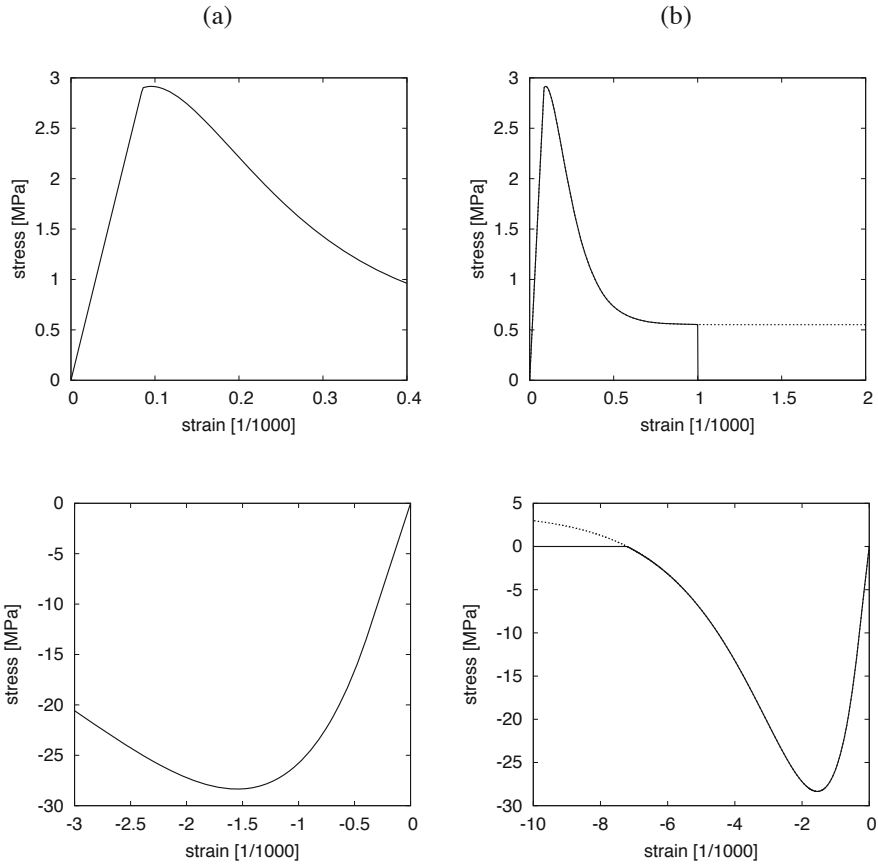

Figure 5. Stress-strain curves for Mazars damage model constructed for uniaxial tension (top) and uniaxial compression (bottom)

where ε_0 is the equivalent strain at the onset of nonlinearity, and A_t, B_t, A_c, and B_c are material parameters related to the shape of the uniaxial stress-strain diagrams. To ensure a continuous variation of slope of the compressive stress-strain curve, it is necessary to satisfy the condition $A_c B_c \varepsilon_0 = A_c - 1$, which reduces the number of independent parameters to four. A sample set of parameters used by Saouridis (1988) is $\varepsilon_0 = 10^{-4}$, $A_t = 0.81$, $B_t = 10450$, $A_c = 1.34$, and $B_c = 2537$. It is important to realize that functions (38)–(39) give a good approximation of the stress-strain curves only in the prepeak and early post-peak regime; see Fig. 5a. For large applied strains the stress level asymptotically approaches its

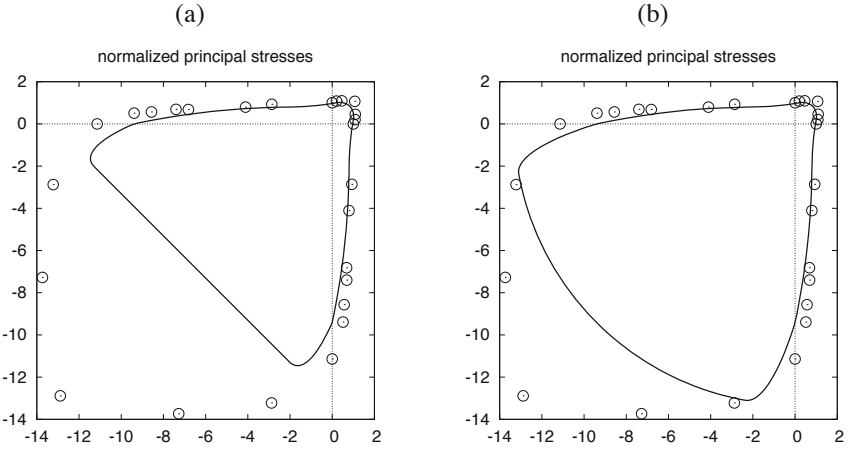

Figure 6. Biaxial failure envelope for Mazars damage model with parameters from Saouridis (1988): a) original version, b) with adjusted equivalent strain according to (41)

limit value $(1 - A_t)E\varepsilon_0$ in tension and $-(1 - A_c)E\varepsilon_0$ in compression. Typically, $A_t < 1$ and $A_c > 1$, and so the stress under uniaxial tension does not completely disappear and under uniaxial compression it changes sign from negative to positive; see the dotted curve in Fig. 5b. This can be remedied by setting $D_c = 1$ when $g_c(\kappa)$ evaluated from (39) exceeds 1, and by setting $D_t = 1$ when κ exceeds a certain limit; see the solid curve in Fig. 5b. Instead of accepting the sudden jump of tensile stress, it is more elegant to modify the definition of g_t such that the tensile stress asymptotically tends to zero. A suitable formula for g_t is e.g.

$$g_t(\kappa) = \begin{cases} 0 & \text{if} \quad \kappa \leq \varepsilon_0 \\ 1 - \dfrac{\varepsilon_0}{\kappa} \exp\left(-\dfrac{\kappa - \varepsilon_0}{\varepsilon_f - \varepsilon_0}\right) & \text{if} \quad \kappa \geq \varepsilon_0 \end{cases} \tag{40}$$

where ε_0 and ε_f are parameters.

The Mazars model allows an independent control of the tensile and compressive stress-strain curves and provides a good approximation of the biaxial failure envelope of concrete (locus of peak stress states under plane stress) under biaxial tension and under tension combined with compression. However the shape of the failure envelope is not realistic in the region of biaxial compression; see Fig. 6a.

A partial improvement of the shape of the failure envelope is obtained if the

equivalent strain is adjusted by the multiplicative factor

$$\gamma = \frac{\sqrt{\sum_{I=1}^{3} (\sigma_I^-)^2}}{\sum_{I=1}^{3} |\sigma_I^-|} \tag{41}$$

where $\sigma_I^- = -\langle -\sigma_I \rangle$ are the negative parts of principal stresses. The adjustment is done only if at least two principal stresses are negative and none of them is positive. In this way, the shape of the failure envelope becomes more realistic; see Fig. 6b. The strength under biaxial compression is now equal to the uniaxial compressive strength. According to the CEB-FIP Model Code (CEB91) it should be by 20% larger but the present version of the model does not allow an independent control of the biaxial compressive strength. For stress paths that do not generate any tensile strains, the model response is purely linear elastic. This means that nonlinear effects under highly confined compression, e.g. the so-called Hugoniot curve under hydrostatic compression, are not reproduced. Note that even though the factor γ in (41) is defined using the nominal stress $\boldsymbol{\sigma}$, exactly the same value is obtained with $\boldsymbol{\sigma}$ replaced by the effective stress $\overline{\boldsymbol{\sigma}} = \mathbb{E} : \boldsymbol{\varepsilon}$, because $\boldsymbol{\sigma} = (1 - D)\overline{\boldsymbol{\sigma}}$ and the factors $1 - D$ appearing both in the numerator and the denominator of (41) cancel out. So the model remains fully explicit in the sense that stresses can be evaluated by straightforward substitution, without any iterations on the material point level.

Mazars model suffers by certain deficiencies that are typical of all isotropic damage models:

1. For a proportional loading path in the stress space the ratio between individual strain components remains constant. Consequently, the model cannot capture the experimentally observed dilatancy (volumetric expansion) at post-peak stages of the uniaxial compression test and of the shear test. Under uniaxial tension, the model predicts unlimited transverse contraction, whereas in reality the transverse strain would approach zero after the formation of a macroscopic crack.
2. When subjected to a large extension in one direction, the model completely loses stiffness not only in the direction of loading but also in the transverse directions.
3. No permanent strain is generated, i.e., unloading takes place to the origin. This could be acceptable for unloading from tension but certainly not for unloading from compression.

Deficiencies 1 and 2 motivate the development of more sophisticated models that take into account the anisotropy induced by damage. Deficiency 3 motivates the development of combined damage-plastic models, to be mentioned in chap-

ter 4. Nevertheless, Mazars model remains quite popular in applications because it is relatively simple, easy to implement, and computationally efficient.

2 Smeared Crack Models

The concept of isotropic damage is appropriate for materials weakened by voids, but if the physical source of damage is the initiation and propagation of microcracks, isotropic stiffness degradation can be considered only as a first rough approximation. More refined damage models take into account the highly oriented nature of cracking, which is reflected by the anisotropic character of the damaged stiffness and compliance matrices.

In this section, we will look at a particular class of constitutive models developed specifically for quasibrittle materials such as concrete or rock under predominantly tensile loading. They will be referred to as smeared crack models (in the narrow sense).

There is some confusion in the literature because the expression "smeared crack" is often perceived as a counterpart of "discrete crack" and, in this sense, any softening continuum model (even if it is based on plasticity or damage) could be labeled as a "smeared crack model". However, we prefer to reserve this term for a more narrow class of models, which share some common features with but are different from plasticity and damage. Similar to plasticity (see chapter 4), they decompose the total strain into an elastic part and an inelastic part (called here the crack strain). Instead of postulating a yield condition and a flow rule, the inelastic strain due to crack opening is related directly to the traction transmitted across the crack plane.

The origins of smeared crack models for concrete fracture date back to the sixties (Rashid, 1968). Initially, the crack direction was assumed to remain fixed, and shear tractions across the crack were treated using the so-called retention factor (Suidan and Schnobrich, 1973). Later, it was proposed to allow rotation of the axes of material orthotropy (Cope et al., 1980), which stimulated the development of rotating crack models (Gupta and Akbar, 1984). The original fixed crack model was later extended to multiple non-orthogonal cracking (de Borst and Nauta, 1985).

As shown by Jirásek and Zimmermann (1998a), the rotating crack model suffers by stress locking (spurious stress transfer), which arises in finite element simulations on meshes that are not aligned with the crack directions. This phenomenon pollutes the numerical results and may lead to a misprediction of structural ductility and of the failure pattern. A remedy based on transition from the rotating crack description to a scalar damage model was proposed in Jirásek and Zimmermann (1998b).

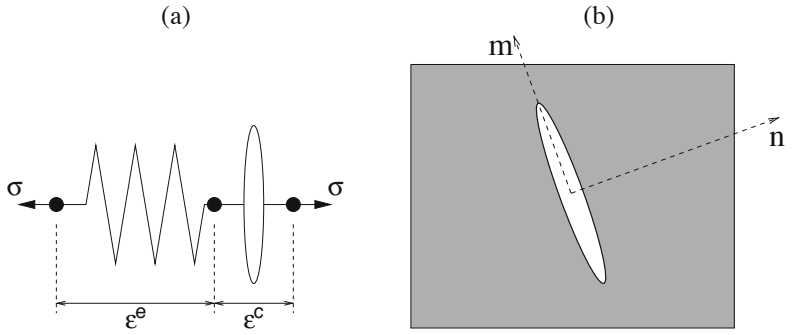

Figure 7. (a) Schematic representation of the smeared crack model as an elastic unit coupled in series to a crack unit, (b) local coordinate system aligned with the crack

2.1 One-Dimensional Smeared Crack Model

Smeared crack models decompose the total strain into two parts — one corresponds to the deformation of the uncracked material, and the other is the contribution of cracking. The response of the uncracked material can be governed by a general nonlinear material law but usually is assumed to be linear elastic. In one-dimensional setting, the strain decomposition is written as

$$\varepsilon = \varepsilon^e + \varepsilon^c \tag{42}$$

and the elastic strain ε^e is related to stress by Hooke's law

$$\sigma = E\varepsilon^e \tag{43}$$

The crack strain, ε^c, represents in a smeared manner the additional deformation due to the opening of cracks. The additive strain decomposition (42) corresponds to a rheological model in which an elastic spring is coupled in series with a unit representing the contribution of the crack, as schematically shown in Fig. 7a. Since the coupling is serial, both units transmit the same stress, σ.

Initially, the material is assumed to be in its virgin (uncracked) state, the crack strain vanishes and the overall response is linear elastic. A crack is initiated when the stress reaches the tensile strength of the material, f_t. A constitutive law governing the stress evolution after crack initiation is needed.

In early studies it was assumed that the traction transmitted by the crack drops to zero immediately after crack initiation. On the structural level, such an approach leads to results that are not objective with respect to the mesh size, as will be explained in Section 3.1. To ensure proper energy dissipation, and also to avoid

unrealistic stress jumps, it is necessary to describe the loss of cohesion as a gradual process. Physically, this is justified by the fact that the formation of a macroscopic stress-free crack is in a heterogeneous material preceded by the initiation, growth and coalescence of a network of microcracks. For the purpose of modeling, we replace such a complicated system of small non-contiguous cracks by an equivalent cohesive crack, which can still transmit stress. This cohesive stress is then considered as a (usually decreasing) function of the crack strain,

$$\sigma = f^c(\varepsilon^c) \tag{44}$$

where the appropriate form of function f^c should be identified from experiments.[3]

Based on a comprehensive analysis of experimental results, Reinhardt et al. (1986) and Hordijk (1991) proposed a softening law in the form

$$\sigma = f^c(\varepsilon^c) \equiv f_t \left\{ \left[1 + \left(\frac{c_1 \varepsilon^c}{\varepsilon_f} \right)^3 \right] \exp\left(-\frac{c_2 \varepsilon^c}{\varepsilon_f} \right) - \mathrm{e}^{-c_2} \left(1 + c_1^3 \right) \frac{\varepsilon^c}{\varepsilon_f} \right\} \tag{45}$$

where f_t is the uniaxial tensile strength, ε_f is the strain at which the crack becomes stress-free, and c_1 and c_2 are dimensionless material parameters controling the shape of the softening curve. Their default values recommended by Hordijk (1991) are $c_1 = 3$ and $c_2 = 6.93$. The corresponding softening curve is plotted in Fig. 8 in terms of dimensionless stress σ / f_t and normalized crack strain $5.136\, \varepsilon^c / \varepsilon_f$ (the factor 5.136 leads to a unit area under the curve). Parameters f_t and ε_f fully define the Reinhardt-Hordijk law with default values of c_1 and c_2, and their change is respectively equivalent to vertical and horizontal rescaling of the normalized curve.

The Reinhardt-Hordijk law (45) gives the best fit of experimental results but is relatively complicated. Acceptable results are usually obtained with simpler relations such as the exponential law

$$\sigma = f^c(\varepsilon^c) \equiv f_t \exp\left(-\frac{\varepsilon^c}{\varepsilon_f} \right) \tag{46}$$

where ε_f is a material parameter controling the steepness of the softening curve,

[3] Due to the localized character of the cracking zone, it is not possible to give an objective definition of the crack strain—it always depends on the gauge length along which the (average) strain is measured. From the physical point of view it is more meaningful to characterize the cracking material by the so-called traction-separation law, which links the cohesive stress transmitted by the crack to the crack opening, defined as the integral of all inelastic deformation across the width of the fracture process zone. This will be discussed in detail in chapter 3.

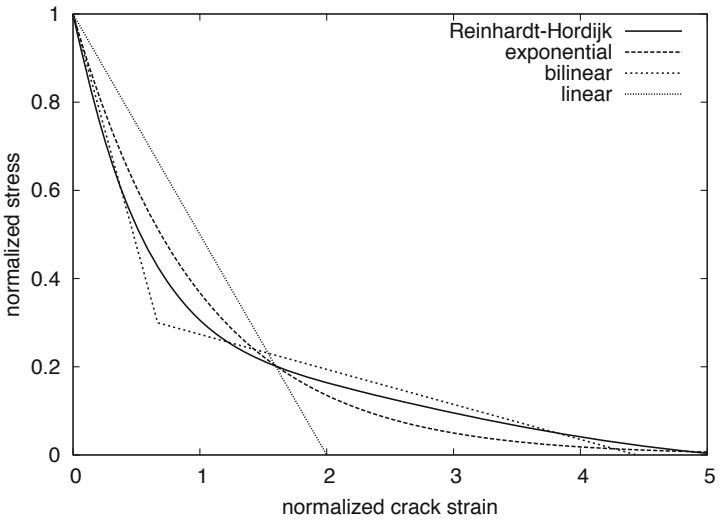

Figure 8. Normalized plot of various softening laws

or the bilinear law

$$\sigma = f^c(\varepsilon^c) \equiv \begin{cases} f_t\left(1 - \dfrac{\varepsilon^c}{\varepsilon_b}\right) + \sigma_b \dfrac{\varepsilon^c}{\varepsilon_b} & \text{if } 0 \le \varepsilon^c \le \varepsilon_b \\ \sigma_b \dfrac{\varepsilon_f - \varepsilon^c}{\varepsilon_f - \varepsilon_b} & \text{if } \varepsilon_b \le \varepsilon^c \le \varepsilon_f \\ 0 & \text{if } \varepsilon_f \le \varepsilon^c \end{cases} \tag{47}$$

where ε_b and σ_b are the coordinates of the point at which the softening curve changes slope, and ε_f is the strain at which the cohesive stress vanishes. The normalized softening curves corresponding to the Reinhardt-Hordijk law (45), exponential law (46) and bilinear law (47) are compared in Fig. 8. The parameters have been determined such that the area under all the curves is equal to unity. It is clear that the deviations of the exponential and bilinear curves from Reinhardt's curve are relatively small. On the other hand, the linear softening curve, also plotted in Fig. 8, substantially differs from the nonlinear ones and, for concrete, can be used only as a very rough approximation.

Equations (42)–(44) fully define the one-dimensional smeared crack model (provided that the strain increases monotonically). The stress-strain curve has a linear pre-peak branch and a softening branch, and for each given stress between 0 and f_t it is easy to compute the corresponding total strain as the sum of the elastic

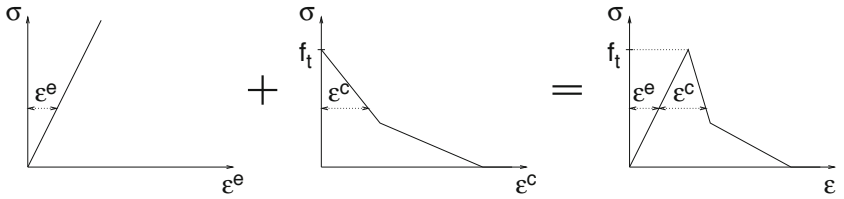

Figure 9. Total stress-strain curve obtained by summing the elastic strain and the crack strain

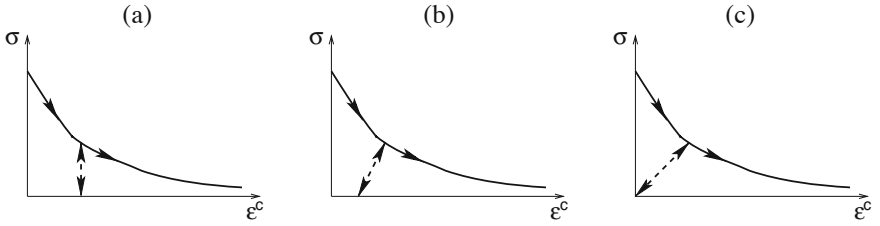

Figure 10. Various types of unloading

strain and the crack strain, as shown in Fig. 9.

Numerical simulations typically require the evaluation of stress for a given strain increment, starting from a state at which all variables are known. For this purpose, the increment of the crack strain must be determined such that the final stress in the elastic spring be equal to the final stress in the cracking unit. This condition leads to the equation

$$E(\varepsilon - \varepsilon^c) = f^c(\varepsilon^c) \tag{48}$$

describing the internal equilibrium in the rheological model in Fig. 7a. Here, ε is the given strain at the end of the step and ε^c is the unknown to be determined. For a linear (or bilinear) softening law, equation (48) is linear (or piecewise linear) and can be solved exactly. For general softening laws such as (45) or (46), the equation is nonlinear and needs to be solved iteratively. Since the functions describing softening are usually smooth and convex, the Newton method leads to very fast monotonic convergence.

For general applications, possible unloading must be taken into account and the cohesive law needs a refinement. The simplest assumption is that unloading is linear. In one extreme case, the crack strain can be considered as permanent, similar to plasticity (Fig. 10a). In another extreme case, perfect crack closure can be assumed, with vanishing crack strain upon complete stress removal (Fig. 10c).

None of these approaches is fully realistic, because crack closure certainly reduces the inelastic part of strain, but it is partially hindered by the roughness of the crack faces and by potential debris inside the cracks (Fig. 10b). Sophisticated models aiming at application to cyclic loading even consider nonlinear unloading, with stiffness recovery upon crack closure and with hysteresis effects. From the computational point of view, the equation to be solved during unloading has the same form as (48), but with a modified function f^c.

To cover the general case, including possible unloading, one should introduce a history variable κ, representing the maximum previously reached value of ε^c, and rewrite (44) as

$$\sigma = f^c(\varepsilon^c, \kappa) \tag{49}$$

The evolution of κ can formally be described by the loading-unloading conditions

$$\varepsilon^c - \kappa \leq 0, \qquad \dot{\kappa} \geq 0, \qquad (\varepsilon^c - \kappa)\,\dot{\kappa} = 0 \tag{50}$$

2.2 Multi-Dimensional Smeared Crack Models

In a general setting, equations (42)–(43) are written as

$$\boldsymbol{\varepsilon} = \boldsymbol{\varepsilon}^e + \boldsymbol{\varepsilon}^c \tag{51}$$

$$\boldsymbol{\sigma} = \mathbb{E} : \boldsymbol{\varepsilon}^e \tag{52}$$

The crack strain, $\boldsymbol{\varepsilon}^c$, represents in a smeared manner the additional deformation due to the opening of cracks. In a real material, microcracks have different sizes, shapes and orientations. They are not necessarily planar and their faces are rough. For the purpose of modeling, simplifications are needed. Therefore, we consider an equivalent computational crack which is perfectly planar and its direction is defined by a unit normal vector $\mathbf{n}$. It is usually assumed that the crack opening and sliding are affected only by the traction vector acting on the crack plane, i.e., by the first-order tensor

$$\mathbf{t}^c = \mathbf{n} \cdot \boldsymbol{\sigma} \tag{53}$$

It is useful to introduce local coordinates aligned with the crack, based on the unit vector $\mathbf{n}$ normal to the crack and on mutually orthogonal unit vectors $\mathbf{m}$ and $\mathbf{l}$ in the crack plane. With respect to such local coordinate system, the traction acting on the crack plane can be represented as

$$\mathbf{t}^c = \sigma_{nn}\mathbf{n} + \sigma_{nm}\mathbf{m} + \sigma_{nl}\mathbf{l} \tag{54}$$

where $\sigma_{nn} = \mathbf{t}^c \cdot \mathbf{n} = \mathbf{n} \cdot \boldsymbol{\sigma} \cdot \mathbf{n}$ is the normal traction and $\sigma_{nm} = \mathbf{t}^c \cdot \mathbf{m} = \mathbf{n} \cdot \boldsymbol{\sigma} \cdot \mathbf{m}$ and $\sigma_{nl} = \mathbf{t}^c \cdot \mathbf{l} = \mathbf{n} \cdot \boldsymbol{\sigma} \cdot \mathbf{l}$ are the shear tractions.

The traction components are linked to the crack opening and sliding by the generalized form of the cohesive law. It is natural to assume that opening of the

crack contributes only to the normal strain ε^c_{nn} in the direction perpendicular to the crack, and sliding of the crack only to the shear strains γ^c_{nm} and γ^c_{nl} in planes perpendicular to the crack. These are the crack strain components expressed with respect to the local coordinate system with unit base vectors $\mathbf{n}$, $\mathbf{m}$ and $\mathbf{l}$. The corresponding strain components in global coordinates are obtained by the standard coordinate transformation. In tensorial notation, we can write

$$\boldsymbol{\varepsilon}^c = \varepsilon^c_{nn}\mathbf{n}\otimes\mathbf{n} + \gamma^c_{nm}(\mathbf{n}\otimes\mathbf{m})_{\text{sym}} + \gamma^c_{nl}(\mathbf{n}\otimes\mathbf{l})_{\text{sym}} = (\mathbf{n}\otimes\mathbf{e}^c)_{\text{sym}} \tag{55}$$

where

$$\mathbf{e}^c = \varepsilon^c_{nn}\mathbf{n} + \gamma^c_{nm}\mathbf{m} + \gamma^c_{nl}\mathbf{l} \tag{56}$$

is the crack strain vector, i.e., a first-order tensor work-conjugate with $\mathbf{t}^c$.

Combining (51), (52) and (55), we obtain the stress-strain law

$$\boldsymbol{\sigma} = \mathbb{E} : (\boldsymbol{\varepsilon} - \mathbf{n}\otimes\mathbf{e}^c) \tag{57}$$

in which $\mathbf{e}^c$ plays the role of an internal variable. Note that, because of minor symmetry of $\mathbb{E}$, the symbol of symmetric part at $\mathbf{n}\otimes\mathbf{e}^c$ can be omitted.

For a virgin material, $\mathbf{e}^c = \mathbf{0}$ and the response is linear elastic. The computational crack is initiated when the stress state reaches the strength envelope, i.e., a certain limit surface in the stress space. Traditional smeared crack models control crack initiation by the Rankine criterion of maximum principal stress. Some models aiming at the description of fracture under shear and compression exploit more general criteria; see e.g. (Weihe, 1995). The initiation criterion should also specify the initial orientation of the crack. For example, the Rankine criterion postulates that, at crack initiation, the crack plane is perpendicular to the direction of maximum principal stress.

Under pure mode-I conditions, the crack propagates in its plane and the normal $\mathbf{n}$ does not change. Under general mixed-mode conditions, two conceptually different approaches are possible:

- Fixed crack models freeze the crack direction and postulate general softening laws that link all crack strain components to all components of the crack traction vector.
- Rotating crack models assume that the crack normal always remains aligned with the current direction of maximum principal strain. The shear components of crack strain, γ^c_{nm} and γ^c_{nl}, and of crack traction, σ_{nm} and σ_{nl}, are then zero, and the simple law (44) with σ and ε^c replaced by σ_{nn} and ε^c_{nn} is sufficient for the description of the softening process.

2.3 Fixed Crack Model

The fixed crack model freezes the crack direction determined at the moment of crack initiation. If the initiation criterion is based on the Rankine condition,

the crack plane initially transmits a normal traction (equal to the tensile strength) but no shear tractions. Later on, the crack plane remains fixed but the principal axes can rotate. The crack plane in general transmits shear tractions that produce relative sliding of the crack faces, represented by shear components of crack strain.

In simplistic versions of the fixed crack model, the shear traction is taken as proportional to the shear crack strain, with a proportionality factor βG, where G is the shear modulus of elasticity and $\beta < 1$ is the so-called shear retention factor (Suidan and Schnobrich, 1973). This is of course not very realistic because such a cohesive crack is allowed to transmit large shear tractions even when it is widely open. If the shear retention factor is treated as a constant, it usually has to be set to a very small value, e.g. $\beta = 0.01$, to limit the spurious stress transfer that could lead to the so-called stress locking.[4] A better remedy is to make β variable, decreasing to zero as the crack opening grows (Cedolin and Poli, 1977). It is also possible to formulate the relation between $\mathbf{t}^c$ and $\mathbf{e}^c$ in the spirit of damage theory, with a scalar damage parameter depending on an equivalent crack strain that is computed from $\mathbf{e}^c$.

Whatever choice is made, the cohesive law can be written in the total form

$$\mathbf{t}^c = \boldsymbol{f}^c(\mathbf{e}^c) \tag{58}$$

or in the rate (incremental) form

$$\dot{\mathbf{t}}^c = \mathbf{E}^c \cdot \dot{\mathbf{e}}^c \tag{59}$$

where $\mathbf{E}^c = \partial \boldsymbol{f}^c / \partial \mathbf{e}^c$ is the second-order tangent crack stiffness tensor.

The traction vector $\mathbf{t}^c$, which is linked by the cohesive law (58) to the crack strain vector $\mathbf{e}^c$, must be equal to the projection of the stress tensor, which can be computed from the elastic strain. Combining equations (53) and (57) we get

$$\mathbf{t}^c = \mathbf{n} \cdot \mathbb{E} : \varepsilon - \mathbf{n} \cdot \mathbb{E} : (\mathbf{n} \otimes \mathbf{e}^c) = \mathbf{n} \cdot \mathbb{E} : \varepsilon - \mathbf{E} \cdot \mathbf{e}^c \tag{60}$$

where $\mathbf{E} = \mathbf{n} \cdot \mathbb{E} \cdot \mathbf{n}$ is the so-called acoustic tensor. Comparing the right-hand sides of (58) and (60), we obtain a generalized form of equation (48), which physically corresponds to the internal equilibrium condition between the tractions in the elastic unit and in the crack unit:

$$\mathbf{n} \cdot \mathbb{E} : \varepsilon - \mathbf{E} \cdot \mathbf{e}^c = \boldsymbol{f}^c(\mathbf{e}^c) \tag{61}$$

For a given strain increment, the unknown crack strain $\mathbf{e}^c$ can be computed by solving (61), which is usually done in an iterative manner, e.g. by the Newton-Raphson method. Substitution of $\mathbf{e}^c$ into (57) then provides the corresponding stress.

[4] In the present context, stress locking means that spurious stresses build up around the band of cracking elements. This pollutes the numerical results and leads to an overestimated energy dissipation and nonzero residual strength of a cracked structure.

It is also useful to derive the tangent material stiffness tensor, which links the stress rate to the strain rate. From the rate form of the internal equilibrium condition (61),

$$\mathbf{n} \cdot \mathbb{E} : \dot{\boldsymbol{\varepsilon}} - \mathbf{E} \cdot \dot{\mathbf{e}}^c = \mathbf{E}^c \cdot \dot{\mathbf{e}}^c \tag{62}$$

the crack strain rate

$$\dot{\mathbf{e}}^c = (\mathbf{E} + \mathbf{E}^c)^{-1} \cdot (\mathbf{n} \cdot \mathbb{E}) : \dot{\boldsymbol{\varepsilon}} \tag{63}$$

is easily computed. Its substitution into the rate form of (57) then gives the rate form of the stress-strain law,

$$\dot{\boldsymbol{\sigma}} = \mathbb{E} : (\dot{\boldsymbol{\varepsilon}} - \mathbf{n} \otimes \dot{\mathbf{e}}^c) = \mathbb{E} : \dot{\boldsymbol{\varepsilon}} - \mathbb{E} : [\mathbf{n} \otimes (\mathbf{E} + \mathbf{E}^c)^{-1}] \cdot (\mathbf{n} \cdot \mathbb{E}) : \dot{\boldsymbol{\varepsilon}} = \mathbb{E}_T : \dot{\boldsymbol{\varepsilon}} \tag{64}$$

with the tangent stiffness tensor of the elastic-cracking material given by

$$\mathbb{E}_T = \mathbb{E} - (\mathbb{E} \cdot \mathbf{n}) \cdot (\mathbf{E} + \mathbf{E}^c)^{-1} \cdot (\mathbf{n} \cdot \mathbb{E}) \tag{65}$$

2.4 Rotating Crack Model

For the rotating crack model (RCM), the plane of the computational crack is allowed to rotate and is assumed to remain perpendicular to the direction of maximum principal strain. Of course, if a physical crack resides in a certain plane, the already formed crack faces cannot rotate. However, if the crack propagates under general loading, it can deviate from the original plane and become non-planar. Also, new cracks in planes that are not parallel with the initial crack plane can be initiated. All this is reflected in the model by a change of direction of the equivalent computational crack.

Alignment of the crack with the principal directions implies that the shear components of the crack strain, γ^c_{nm} and γ^c_{nl}, are zero. Equation (56) then simplifies to $\mathbf{e}^c = \varepsilon^c_{nn}\mathbf{n}$ and (57) turns into

$$\boldsymbol{\sigma} = \mathbb{E} : (\boldsymbol{\varepsilon} - \mathbf{N}\varepsilon^c_{nn}) \tag{66}$$

where, for convenience, the second-order tensor $\mathbf{n} \otimes \mathbf{n}$ is denoted as $\mathbf{N}$. The normal traction on the crack plane can be evaluated by an appropriate projection of the stress tensor:

$$\sigma_{nn} = \mathbf{n} \cdot \boldsymbol{\sigma} \cdot \mathbf{n} = \mathbf{N} : \boldsymbol{\sigma} = \mathbf{N} : \mathbb{E} : \boldsymbol{\varepsilon} - \mathbf{N} : \mathbb{E} : \mathbf{N}\varepsilon^c_{nn} \tag{67}$$

At the same time, this traction is linked to the normal crack strain, ε^c_{nn}, by a scalar cohesive law analogous to (44):

$$\sigma_{nn} = f^c(\varepsilon^c_{nn}) \tag{68}$$

Comparing the right-hand sides of (67) and (68), we obtain the internal equilibrium condition

$$\mathbf{N} : \mathbb{E} : \boldsymbol{\varepsilon} - \mathbf{N} : \mathbb{E} : \mathbf{N}\varepsilon_{nn}^c = f^c(\varepsilon_{nn}^c) \tag{69}$$

which is analogous to (61) but is simpler, with only one scalar unknown ε_{nn}^c instead of the vectorial unknown $\mathbf{e}^c$.

If the uncracked material is isotropic, the elastic stiffness is given by $\mathbb{E} = \lambda \mathbf{1} \otimes \mathbf{1} + 2\mu \mathbb{I}_S$ where λ and μ are Lamé's constants and $\mathbb{I}_S$ is the symmetric fourth-order unit tensor. In this case, we have $\mathbf{N} : \mathbb{E} = \lambda \mathbf{1} + 2\mu \mathbf{N}$ and $\mathbf{N} : \mathbb{E} : \mathbf{N} = \lambda + 2\mu$, and (69) can be written as

$$\lambda \mathbf{1} : \boldsymbol{\varepsilon} + 2\mu \mathbf{N} : \boldsymbol{\varepsilon} - (\lambda + 2\mu)\varepsilon_{nn}^c = f^c(\varepsilon_{nn}^c) \tag{70}$$

where $\mathbf{1} : \boldsymbol{\varepsilon}$ is the trace of the strain tensor and $\mathbf{N} : \boldsymbol{\varepsilon} = \mathbf{n} \cdot \boldsymbol{\varepsilon} \cdot \mathbf{n}$ is the (total) strain normal to the crack, which is in fact equal to the maximum principal strain. Similar to the one-dimensional case, the crack strain ε_{nn}^c can be obtained by the Newton method (or in closed form, if the softening law is linear or piecewise linear). Substitution of the result into (66) then provides the stress tensor.

In order to derive the tangent stiffness tensor for the rotating crack model, we first convert the internal equilibrium equation (70) to the rate form. It is important to realize that the crack normal $\mathbf{n}$ in general rotates, and so the second-order tensor $\mathbf{N} = \mathbf{n} \otimes \mathbf{n}$ is also variable in time. This needs to be taken into account when differentiating the second term in (70). The resulting rate equation thus reads

$$\lambda \mathbf{1} : \dot{\boldsymbol{\varepsilon}} + 2\mu \mathbf{N} : \dot{\boldsymbol{\varepsilon}} + 2\mu \dot{\mathbf{N}} : \boldsymbol{\varepsilon} - (\lambda + 2\mu)\dot{\varepsilon}_{nn}^c = E^c \dot{\varepsilon}_{nn}^c \tag{71}$$

where $E^c = \mathrm{d}f^c/\mathrm{d}\varepsilon_{nn}^c$ is the softening modulus. The rates $\dot{\mathbf{n}}$ and $\dot{\mathbf{N}}$ can be expressed in terms of the current strain and the strain rate, but the derivation is somewhat tedious. As explained in the footnote,[5] $\dot{\mathbf{N}} = \mathbb{N} : \dot{\boldsymbol{\varepsilon}}$ where $\mathbb{N}$ is a certain fourth-order tensor depending only on $\boldsymbol{\varepsilon}$ and $\mathbf{n}$. It can be shown that $\mathbb{N} : \boldsymbol{\varepsilon} = \mathbf{O}$, and thus the the third term in (71) cancels.

[5] According to the fundamental assumption of the rotating crack model, the crack remains perpendicular to the direction of maximum principal strain, i.e., $\mathbf{n} = \mathbf{p}_1$ is the normalized eigenvector of $\boldsymbol{\varepsilon}$ associated with the largest eigenvalue. If the maximum principal strain ε_1 is strictly greater than the other two principal strains, ε_2 and ε_3, the expression for the rate of $\mathbf{p}_1$ can be derived by manipulating the rate form of the relations $\boldsymbol{\varepsilon} \cdot \mathbf{p}_I = \varepsilon_I \mathbf{p}_I$ and $\mathbf{p}_I \cdot \mathbf{p}_J = \delta_{IJ}$, $I, J = 1, 2, 3$. The resulting formula reads

$$\dot{\mathbf{p}}_1 = \frac{\dot{\varepsilon}_{12}\mathbf{p}_2}{\varepsilon_1 - \varepsilon_2} + \frac{\dot{\varepsilon}_{13}\mathbf{p}_3}{\varepsilon_1 - \varepsilon_3} \tag{72}$$

where $\dot{\varepsilon}_{12} = \mathbf{p}_1 \cdot \dot{\boldsymbol{\varepsilon}} \cdot \mathbf{p}_2$ and $\dot{\varepsilon}_{13} = \mathbf{p}_1 \cdot \dot{\boldsymbol{\varepsilon}} \cdot \mathbf{p}_3$ are the components of the strain rate tensor $\dot{\boldsymbol{\varepsilon}}$ with respect to the principal coordinate system. It is then straightforward to evaluate $\dot{\mathbf{N}} = \dot{\mathbf{p}}_1 \otimes \mathbf{p}_1 + \mathbf{p}_1 \otimes \dot{\mathbf{p}}_1$ and convert it to the form $\dot{\mathbf{N}} = \mathbb{N} : \dot{\boldsymbol{\varepsilon}}$ where

$$\mathbb{N} = \frac{2}{\varepsilon_1 - \varepsilon_2}(\mathbf{p}_1 \otimes \mathbf{p}_2)_{\text{sym}} \otimes (\mathbf{p}_1 \otimes \mathbf{p}_2)_{\text{sym}} + \frac{2}{\varepsilon_1 - \varepsilon_3}(\mathbf{p}_1 \otimes \mathbf{p}_3)_{\text{sym}} \otimes (\mathbf{p}_1 \otimes \mathbf{p}_3)_{\text{sym}} \tag{73}$$

Based on (71) with the third term dropped, the crack strain rate corresponding to a given strain rate is easily expressed as

$$\dot{\varepsilon}^c_{nn} = \frac{\lambda \mathbf{1} : \dot{\boldsymbol{\varepsilon}} + 2\mu \mathbf{N} : \dot{\boldsymbol{\varepsilon}}}{\lambda + 2\mu + E^c} = \frac{\mathbf{N} : \mathbb{E}}{\lambda + 2\mu + E^c} : \dot{\boldsymbol{\varepsilon}} \tag{74}$$

Substitution of this result into the rate form of (66) leads to the direct relation between the rates of stress and strain,

$$\dot{\boldsymbol{\sigma}} = \mathbb{E} : (\dot{\boldsymbol{\varepsilon}} - \dot{\mathbf{N}}\varepsilon^c_{nn} - \mathbf{N}\dot{\varepsilon}^c_{nn}) = \mathbb{E} : \dot{\boldsymbol{\varepsilon}} - \mathbb{E} : \mathbb{N} : \dot{\boldsymbol{\varepsilon}}\, \varepsilon^c_{nn} - \mathbb{E} : \mathbf{N} \frac{\mathbf{N} : \mathbb{E}}{\lambda + 2\mu + E^c} : \dot{\boldsymbol{\varepsilon}} \tag{75}$$

This can be further simplified, since $\mathbb{E} : \mathbb{N} = 2\mu\mathbb{N}$ (as follows from (73)). The final formula for the tangent stiffness tensor reads

$$\mathbb{E}_T = \mathbb{E} - 2\mu\varepsilon^c_{nn}\mathbb{N} - \frac{\mathbb{E} : \mathbf{N} \otimes \mathbf{N} : \mathbb{E}}{\lambda + 2\mu + E^c} \tag{76}$$

The rotating crack model is probably the simplest model that can take into account cracking-induced anisotropy within a framework close to continuum damage mechanics. Nevertheless, let us point out that it has a number of drawbacks, analyzed in detail by Rots (1988) and Jirásek and Zimmermann (1998a). For instance, it is not thermodynamically consistent. This can be demonstrated by looking at formula (76) for the tangent stiffness. Its derivation is valid not only in the case of crack growth, but also during unloading (with constant positive modulus E^c), when the pre-cracked material should respond as an anisotropic linear elastic one, and it should be characterized by a constant and positive definite tangent stiffness. However, formula (76) indicates that the stiffness tensor remains constant only if tensors $\mathbf{N}$ and $\mathbb{N}$ remain constant, i.e., if the principal axes do not rotate. As shown by Jirásek and Zimmermann (1998a), under certain circumstances the unloading stiffness can even lose positive definiteness, which leads to nonphysical instabilities.

2.5 Rotating Crack Model with Transition to Scalar Damage

In applications to failure simulation by the finite element method, it is necessary to avoid stress locking, which arises on meshes not aligned with the crack directions and is caused by the poor kinematic representation of the discontinuous displacement field around a macroscopic crack. This leads to spurious stress transfer, which pollutes the numerical results and may result into a misprediction of structural ductility and of the failure pattern.

A typical example of stress locking in a fracture simulation is presented in Fig. 11. A three-point bend specimen (Fig. 11a) is discretized by constant-strain triangular elements. The macroscopic crack is initiated at the notch tip and propagates

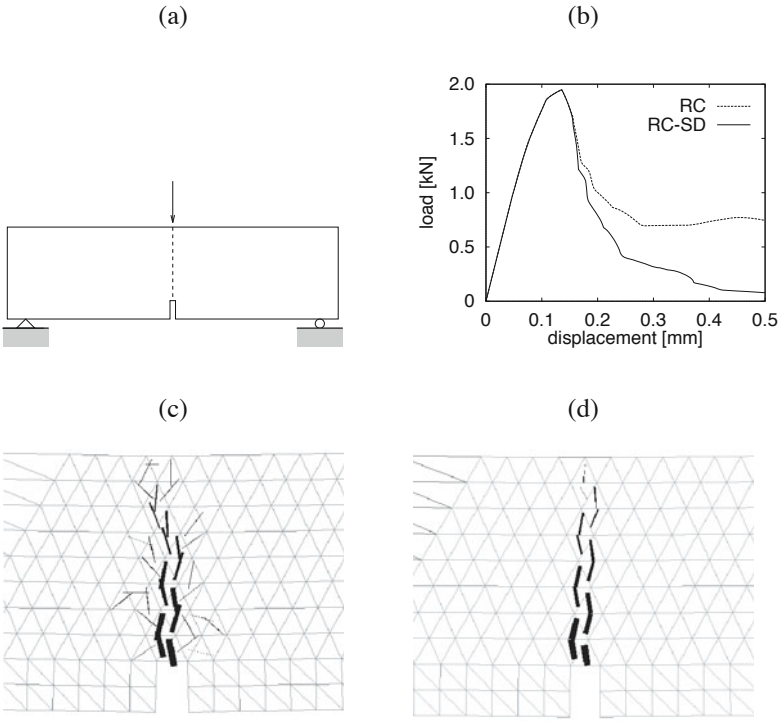

Figure 11. Three-point bending test: a) geometry and loading, b) load-displacement curves, c) crack pattern for the RC model, d) crack pattern for the RC-SD model

across the specimen. After a sufficiently large load-point displacement has been applied, the specimen should break completely, and the resisting force should vanish. However, the post-peak branch of the computed load-displacement diagram does not tend to zero but to a non-negligible residual value of the resisting force, which then remains roughly constant, or even slightly increases (dashed curve in Fig. 11b). This is indeed a paradoxical result since strains in the cracking elements are no doubt sufficiently large to make the corresponding stresses vanish. The stress-strain law is designed in such a way that the stress transfered across a crack is zero as soon as the crack opening reaches a certain critical value. For the fixed crack model with non-zero retention factor (Rots, 1988), stress locking occurs due to shear stresses transfered across the crack. The rotating crack model does not produce any shear stress on the crack faces but it still locks. The origin